Computing the Soret coefficient in aqueous mixtures using boundary driven nonequilibrium molecular dynamics

ARTICLE *in* THE JOURNAL OF CHEMICAL PHYSICS · APRIL 2005

Impact Factor: 2.95 · DOI: 10.1063/1.1863872 · Source: PubMed

3 AUTHORS, INCLUDING:

Josep Bonet Avalos
Universitat Rovira i Virgili

70 PUBLICATIONS **1,207** CITATIONS

SEE PROFILE

Computing the Soret coefficient in aqueous mixtures using boundary driven nonequilibrium molecular dynamics

Carlos Nieto-Draghi and Josep Bonet Ávalos
Departament d'Enginyeria Química, ETSEQ, Universitat Rovira i Virgili, Auinguda dels Països Catalans 26, 43007 Tarragona, Spain

Bernard Rousseau
Laboratoire de Chimie-Physique, Bâtiment 350, Université Paris-Sud, 91405 Orsay Cedex, France

(Received 20 December 2004; accepted 7 January 2005)

We have computed the Soret coefficient in aqueous mixtures using a boundary driven nonequilibrium molecular dynamics algorithm and standard molecular force fields. The choice of this specific approach is justified by the nature of the mixtures studied here. Four aqueous solutions, including methanol, ethanol, acetone, and dimethyl-sulfoxide (DMSO) have been studied at ambient conditions for different compositions. The experimental behavior of water-alcohol mixtures was reproduced, including the change of sign of the Soret coefficient with composition, in excellent agreement with existing experimental data. The methodology has been applied to obtain pure predictions for water-acetone and water-DMSO where no experimental data are accessible. A change of sign is also observed in the same range of composition as in water-alcohol mixtures. It is suggested that the nature and strength of the molecular interactions, rather than the mass or shape ratio of the components, dominates the behavior of the Soret coefficient versus composition for the aqueous associating mixtures studied here. © *2005 American Institute of Physics*. [DOI: 10.1063/1.1863872]

I. INTRODUCTION

The thermal diffusion effect refers to the appearance of a composition gradient in a mixture under a temperature gradient, in the absence of convection. This effect is also known as Soret effect or Ludwig–Soret effect in liquids. In the framework of nonequilibrium thermodynamics the Soret effect is considered as a *crossed effect* in the sense that a gradient of composition is caused by a heat flow and, ultimately, by a temperature gradient.

Although this effect is usually small, it has interesting applications such as the separation of isotopes. However, the microscopic origin of this effect, related to the masses of the molecules of the mixture, the chemical interactions between them and also on the shape of the particles, is not completely understood. In this paper we will analyze the Soret effect in liquid mixtures of associating fluids, such as water and ethanol, where the Soret effect is believed to be determined by the strong interparticle interactions. Our method of analysis is the application of *boundary driven* nonequilibrium molecular dynamics simulations, which we prove to have a quantitative predicting character, able to produce new values for the Soret coefficients in some of the studied mixtures.

The intensity of the thermal diffusion effect is described by the thermal diffusion factor α_T. The sign of α_T has a very important meaning: it reflects the direction of separation of the components of the mixture when a thermal gradient is applied. For a binary mixture, α_T is defined as

$$\alpha_T = -\frac{T}{w_1 w_2}\frac{\nabla w_1}{\nabla T}, \tag{1}$$

where T is the temperature and w_i the mass fraction of species i. The thermal diffusion effect is usually a small effect. The thermal diffusion factor depends on temperature, pressure, and composition. At low pressure, the thermal diffusion factor of gaseous mixtures is roughly independent of the composition. Indeed, the kinetic theory of gases predicts that the thermal diffusion factor in gases is mostly determined by molecular mass or size ratio between species in the mixture.[1] In liquids, the energetic interactions, the size, and the shape of molecules are the main parameters. Debuschewitz and Köhler[2] have shown that the Soret coefficient can be split into independent contributions: a mass effect, depending on the mass and moment of inertia difference of the species, and what they call the chemical effect. The mass effect is found to be independent of composition, while the composition effect comes solely from the chemical part. In ideal and nearly ideal mixtures, the thermal diffusion factor is slightly dependent of the composition. This has been observed, e.g., for rare gas mixtures[3] and alkanes.[4] The situation is quite different in strongly nonideal or associating mixtures, where a change of sign in the thermal diffusion factor with composition is almost invariably observed. The effect of nonideality and association on thermal diffusion in aqueous mixtures was extensively studied during the 1950s by Drickamer[5] or Prigogine.[6,7] A detailed presentation of results before 1961 is given in Tyrrell book.[8]

In the recent years, there has been a renewed interest in the thermal diffusion effect for such mixtures. Kolodner[9]

published a detailed experimental work on the thermal diffusion of water-ethanol mixtures, using a laser-beam-deflection technique. He observed that the change in the sign of the coefficient was always independent of the average temperature of the experiments and that always occurred in a range of molar fraction of ethanol between $x_{et}=0.1$ and $x_{et}=0.25$. Piazza and collaborators recently published the results of a set of experiments employing also a laser-beam-deflection technique, in which a charged colloid suspension presented a strong concentration dependence as well as temperature dependence of the Soret coefficient. In this case, the sign of α_T can be tuned by varying the Debye–Huckel screening length[10–12] by changing the ion concentration in a NaCl solution. Similarly, Wiegand and collaborators employed a thermal diffusion Rayleigh scattering technique to study colloidal suspensions of poly(ethylene oxide) in water-ethanol mixtures,[13–17] finding that the migration of colloidal particles is linked to the migration of the best solvent in the solution. Although kinetic theory of gas enables accurate calculation of α_T in gas mixtures, the accuracy of the methods to predict α_T in liquids or dense fluids reported up to date in the literature, is very limited, especially when dealing with associating mixtures.[5–7,18–22]

The new and accurate experimental data obtained on associated mixtures or polymer and colloidal suspensions, motivate further work to understand the process of thermal diffusion from a theoretical point of view. The particular behavior observed for α_T with composition in associating mixtures raises the question of the role played by intermolecular interactions in this phenomenon. It is then of particular interest the analysis of the problem through molecular simulation since this method permits a complete control on the behavior of the system at a microscopic level, especially in the interpretation of the microscopic causes of the macroscopically observed phenomenon under discussion in this work. Thanks to the development of efficient algorithms, accurate force fields, and the increase of computer speed, molecular dynamics has become a powerful tool for the prediction of transport properties in fluid mixtures. However, in the particular, but especially interesting, case of strongly nonideal mixtures or associating fluids, some care must be taken in the computation of the thermal diffusion factor using molecular dynamics. In a short paper, we have reported some predictions for the values of the thermal diffusion factor for aqueous solutions of associating fluids.[23] In the present work, we have employed a *boundary driven* nonequilibrium molecular dynamics method and conventional force fields to compute the thermal diffusion factor in aqueous mixtures, namely, binary mixtures of water with methanol, ethanol, dimethyl sulfoxide (DMSO), and acetone. This method is presented here in detail and is validated for such kind of mixtures by comparison with experimental data on several water-alcohol mixtures.

The present paper is organized as follows. In Sec. II, the general methodology used in this work for the computation of the thermal diffusion factor in associating mixtures is presented. In Sec. III, we give some details on the computational aspects of this work. Nonequilibrium molecular dynamics data are presented in Sec. IV. Finally, Sec. V addresses the concluding remarks on this work.

II. METHODOLOGICAL ASPECTS

The mass flux in a binary mixture under a thermal gradient is governed by the simultaneous action of a separation effect, caused by the thermal gradient, and a mixing effect, caused by mutual diffusion between different species. As such, the constitutive equation for the mass flux in a center of mass reference frame is given by[8]

$$\mathbf{J}_1 = -\rho w_1 w_2 D_T \nabla T - \rho D \nabla w_1, \tag{2}$$

where ρ is the density of the mixture, D is the mutual diffusion coefficient, and D_T is the thermal diffusion coefficient, which couples the mass flow with the thermal gradient. At the stationary state in a closed system, the two effects have to counterbalance so that the mass flux is zero. The Soret coefficient is then defined as

$$S_T = D_T/D = -\left(\frac{1}{w_1 w_2}\frac{\nabla w_1}{\nabla T}\right)_{\mathbf{J}_1=0}. \tag{3}$$

The thermal diffusion factor α_T is simply defined as TS_T. The macroscopic relation, Eq. (2), describing the transport of matter in a two-component mixture can also be expressed, in the framework of nonequilibrium thermodynamics, as[24]

$$\mathbf{J}_1 = -L_{1q}\frac{\nabla T}{T^2} - L_{11}\frac{\mu_{11}^w}{w_2 T}\nabla w_1. \tag{4}$$

Here, μ_{11}^w is the derivative of the chemical potential of species 1 relative to w_1 and the L_{ij} are the so-called *phenomenological* Onsager coefficients, describing the proportionality between fluxes and thermodynamic forces. From Eq. (4), an expression of S_T in terms of the L_{ij}'s can be given at the stationary state:

$$S_T = -\left(\frac{1}{w_1 \mu_{11}^w T}\frac{L_{1q}}{L_{11}}\right)_{\mathbf{J}_1=0}. \tag{5}$$

Equations (3) and (5) intrinsically express two different ways to obtain the thermal diffusion factor using molecular dynamics simulations. One route through Eq. (3) consists on simulating the situation occurring in a real experiment, i.e., by introducing a thermal gradient (or imposing a heat flux) in the simulation box. Such methods are classified as boundary driven nonequilibrium molecular dynamics methods (BD-NEMD). The other route through Eq. (5) consists on directly computing the Onsager coefficients L_{ij} using equilibrium molecular dynamics simulations (EMD) and the Green–Kubo formalism, or the *synthetic* nonequilibrium molecular dynamics (S-NEMD) algorithms proposed by Evans or Ciccotti.

The route through the phenomenological Onsager coefficients L_{ij} has been employed by Vogelsang *et al.*[25,26] using EMD and the Green–Kubo formalism. Evans and co-workers[27–29] and Ciccotti and co-workers[30] proposed different algorithms based on the linear response theory. However, one crucial point in the determination of S_T through the computation of L_{ij} is that additional quantities are needed to

relate the L_{ij} to the experimentally accessible S_T, namely, the value of the thermodynamic factor μ_{11}^w, according to Eq. (5). For isotopic or nearly ideal mixtures, one can use the ideal value for μ_{11}^w as a first approximation. Jolly and Bearman[31] and Schoen and Hoheisel[32] obtained μ_{11}^w from simulations by integration of pair correlation functions. However, Stoker and Rowley[33] argued that it is very difficult to obtain reliable statistics using this method and these authors preferred to obtaind estimated values for μ_{11}^w given by the UNIFAC method. It was shown by Tichacek, Kmak, and Drickamer[5] that the actual values of $w_1\mu_{11}^w$ for a nonideal mixture can differ from the ideal values, and that this fact strongly affects the final value of the Soret coefficient. Moreover, $w_1\mu_{11}^w$ tends to zero close to the critical point, which causes in addition S_T to diverge in this region of the phase diagram. Consequently, the reliability of the values of $w_1\mu_{11}^w$ is the main problem in the computation of the Soret coefficient in nonideal mixtures.

Other thermodynamic quantities also appear in the expression of L_{1q}, because the heat flux J_q is not directly accessible by molecular simulation in the case of mixtures. Only the internal energy flux J_U, given by Irving and Kirkwood,[34] can be expressed in terms of microscopic quantities. For a binary mixture, one has

$$J_q - J_U - (h_1 - h_2)J_1, \tag{6}$$

where h_i is the partial molar enthalpy of species i. Again, one may use the ideal mixture expression for the h_i, as a first approximation, use simulations to evaluate the values of these partial molar enthalpies (with all the accuracy problems also mentioned for μ_{11}^w), or resort to empirical correlations and experimental data.

However, one can avoid the computation of thermodynamics quantities by using BD-NEMD. In this work, we have obtained predictions of the Soret coefficient by using the boundary driven *reverse* NEMD algorithm from Müller–Plathe,[35] also referred to as PeX algorithm, with modifications to account for holonomic constraints[36] in molecular models, as well as to treat molecules with different masses.[37]

In our BD-NEMD two slabs of a given thickness, large enough to contain a sufficiently large number of particles on average but much smaller than the total length of the box in the z direction, are created. In order to create a heat flux in the z direction, a particle with the highest kinetic energy in the so-called *cold* slab is selected, with frequency ν, to experiment a hypothetical elastic collision with the particle having the lowest kinetic energy in the *hot* slab.[37] After such a virtual collision the two particles have changed their velocity without change in their respective location in space. The new velocity of the molecule in the cold region can be expressed as[38]

$$\mathbf{v}_c^{\text{new}} = -\mathbf{v}_c^{\text{old}} + 2\frac{m_c\mathbf{v}_c^{\text{old}} + m_h\mathbf{v}_h^{\text{old}}}{m_c + m_h} \tag{7}$$

while, for the molecule in the hot region,

$$\mathbf{v}_h^{\text{new}} = -\mathbf{v}_h^{\text{old}} + 2\frac{m_c\mathbf{v}_c^{\text{old}} + m_h\mathbf{v}_h^{\text{old}}}{m_c + m_h}, \tag{8}$$

where m_c and m_h are the respective masses of the particles selected in the cold and hot slabs, $\mathbf{v}_h^{\text{new}}$ and $\mathbf{v}_h^{\text{old}}$ stand, respectively, for the velocities of the particle after and before the collision. During the elastic collision the particles exchange their momentum. In this scheme, the total momentum and energy of the system are kept constant. Moreover, the simulation box has periodic boundary conditions in the three dimensions of space.

The kinetic energy exchanged by means of these elastic collisions are used to compute the energy flux in the system. The heat flow density at steady state is thus given by the relation

$$\langle J_z\rangle_\tau = \frac{1}{2A\tau}\sum_{\text{transfers}}\frac{m_h}{2}(\mathbf{v}_h^{\text{new }2} - \mathbf{v}_h^{\text{old }2}). \tag{9}$$

In this expression, A is the cross sectional area, τ is the time interval of measure at the stationary state during which a given number of momenta transfers have occurred, and $\langle J_z\rangle_\tau$ is the heat flux in the z direction, which can be indistinctly evaluated at the cold or hot slab. It is required that the number of particles in both slabs is sufficiently large in order to that the collisions inside the slabs will properly thermalize the velocity distribution before a new collision takes place. At the stationary state, the thermal diffusion factor can be obtained using Eq. (1). The composition and thermal gradients are obtained from a linear fit of local concentration and temperature profiles rising from the simulation.

III. COMPUTATIONAL DETAILS

There have only been a few attempts to compute the Soret coefficient in molecular liquids using molecular dynamics simulations. Schaink and co-workers[39,40] studied cyclohexane-benzene mixtures and CF_4–CH_4 mixtures. However, they were not able to reduce the statistical error below 50% and meaningful comparisons with theoretical or experimental data were thus not possible. Latter, and using a parallel computer, Simon *et al.*[41,42] used BD-NEMD to compute the thermal diffusion factor in alkanes binary mixtures. Perronace *et al.* computed Soret coefficients in argon-krypton mixtures[43] and *n*-pentane-*n*-decane[4] mixtures using both EMD, S-NEMD and BD-NEMD simulations. Their results were compared to experimental data and gave a satisfactory agreement.

In this work, we present simulation results for thermal diffusion in aqueous mixtures using standard molecular models. In water-alcohol simulations, we employed the OPLS (Ref. 44) models for methanol and ethanol, and the TIP4P model for water.[45] These models are well known and have been employed for studying thermodynamics[46,47] as well as transport properties.[48–52] In the case of the water-DMSO we have used the P2 model of Luzar and Chandler[53] for the DMSO (where methyl groups were treated as united atoms), and the SPC/E (Ref. 54) model to simulate water molecules. The use of these models is supported by previous work[55,56] on self-diffusion, dielectric properties, and shear viscosity[57]

TABLE I. Potential parameters of the models used in this work. For more details about the models see Ref. 44, 45, 53, 54, and 58.

Site	σ (Å)	ϵ (kJ/mol)	Charge (e)
	Water (SPC/E)[a]		
O	3.165 648	0.650 167	−0.8476
H	0.0	0.0	0.4238
	Water (TIP4P)[b]		
O	0.153 577 9	0.648 694 3	0.00
H	0.0	0.0	0.52
M	0.0	0.0	−1.04
	Methanol (OPLS)[c]		
O(COH)	3.07	0.711 756	−0.700
H	0.0	0.0	0.435
CH_3	3.775	0.866 668	0.265
	Ethanol (OPLS)[c]		
O(COH)	3.07	0.711 756	−0.700
H	0.0	0.0	0.435
CH_2	3.905	0.493 712	0.265
CH_3	3.905	0.732 200	0.0
	DMSO (P2)[d]		
S	3.4	0.997 41	0.139
O	2.8	0.299 22	−0.459
CH_3	3.8	1.230	0.160
	Acetone[e]		
O	3.01	0.706 69	−0.540
C	3.78	0.415 70	0.48
CH_3	3.88	0.681 748	0.03

[a]Reference 54.
[b]Reference 45.
[c]Reference 44.
[d]Reference 53.
[e]Reference 58.

at ambient conditions, where good agreement with experimental data has been observed. Finally, for the water-acetone system we employed the SPC/E model for water molecules and the model of Wheeler and Rowley[58] for the acetone molecules. The potential parameters of the different models employed are given in Table I.

All molecular models considered in this work have been treated as composed of several Lennard–Jones sites plus point charges, according to

$$U_{ij} = 4\epsilon_{ij}\left[\left(\frac{\sigma_{ij}}{r_{ij}}\right)^{12} - \left(\frac{\sigma_{ij}}{r_{ij}}\right)^{6}\right] + \frac{q_i q_j}{4\pi\epsilon_0 r_{ij}}, \tag{10}$$

where q_i is the partial charge on site i, ϵ_{ij} and σ_{ij} are the Lennard–Jones interaction parameters between sites i and j on different molecules, and r_{ij} being the separation distance between sites i and j. Crossed interactions were computed through Lorentz–Berthelot rules for water-DMSO and water-acetone, while geometric average has been employed for the OPLS models in the water-alcohol systems.[44] All the simulations have been performed with periodic boundary conditions and the *reaction field* methodology[59] with the choice $\epsilon_{RF}=\infty$, to account for the long-range electrostatic interactions.

BD-NEMD simulations were carried out with 500 molecules for the water-DMSO and water-acetone systems, whereas 800 molecules have been employed for water-methanol and water-ethanol systems. A parallelepipedic box was employed with the particular choice of $l_z=2l_x=2l_y$, where l_x, l_y, l_z are the dimensions of the simulation cell. The equations of motion were integrated with a time step of 2 fs. The reaction field and Lennard–Jones cutoff length is 10.26 Å, and a nearest neighbor list technique,[60] with a cutoff radius of 11.1 Å, has been also employed. Each simulation run lasted at least 25 ns, although for some water-alcohol systems, 100 ns was employed.

We used a collision frequency (momentum transfer between hot and cold slabs) of $\nu=0.0025$ fs^{-1} to generate the heat flux and thermal gradient. In all cases, compositions and cell dimensions were chosen to reproduce the experimental density of the mixture at 298 K and 1 atm at the same composition (water-methanol was studied at 313.15 K). Compositions and densities are summarized in Table II. For each studied state, a preliminary run of roughly 500 ps was performed to reach a stationary state characterized by linear temperature and concentration profiles. Such profiles can be seen in Fig. 1 for water-methanol, and are similar in all the other cases. As can be seen in this figure, although larger fluctuations in composition profiles than in temperature profiles occur, the profiles can be considered as linear as a good approximation. The temperature gradient ∇T and water mole fraction gradient ∇x_w were obtained from the slope of a linear regression of the simulation data. Additionally, in Fig. 2 it is possible to observe a transient heat flux across the simulation box until the steady state is reached at around 500 ps. Our choice of an equilibration period of about 500 ps to have linear profiles is consistent with the duration of this transient behavior.

IV. RESULTS AND DISCUSSION

In this section, we present the simulation results for the thermal diffusion factor of the four mixtures analyzed.

In Fig. 3, we present the variation of the thermal diffusion factor for the water-methanol mixture versus composition at 313 K and 1 atm. Our simulations are compared with the experimental data of Tichacek, Kmak, and Drickamer under the same thermodynamic conditions. We find a good agreement between the experimental and simulation results, taking into account that our simulation data present large statistical errors of about 30% (similar to the accuracy also reached in previous calculations of the Soret coefficient in other mixtures[4,41,42]), which is of the order, however, of the confidence range of the experimental data. We consider that the agreement between experimental and simulation results is thus remarkable, specially if one takes into account that the change of sign of the coefficient with composition has been clearly reproduced. The change in the sign of the Soret coefficient is observed between 80% and 95% molar concentration of water for both experiments and simulations. Contrary to mixtures of nonassociating fluids, where a weak concentration dependence of thermal diffusion is observed (for example, mixtures of *n*-pentane and *n*-decane[4]), α_T in water

TABLE II. Simulated thermodynamic states. All data at 298 K and 1 atm except for water-methanol system at 313.15 K and 1 atm. Experimental densities were taken from the following references: water-methanol (Ref. 64), water-ethanol (Ref. 61), water-DMSO (Ref. 65), water-acetone (Ref. 66). Thermal diffusion factor α_T is a dimensionless quantity.

	Mole fractions						
State	Water	Methanol	Ethanol	DMSO	Acetone	ρ (q/cm^3)	α_T
1	0.875	0.125	⋯	⋯	⋯	0.9473	+1.19±0.60
2	0.773	0.227	⋯	⋯	⋯	0.9171	−1.29±0.60
3	0.505	0.495	⋯	⋯	⋯	0.8519	−0.84±0.63
4	0.36	0.64	⋯	⋯	⋯	0.8273	−0.83±0.65
5	0.95	⋯	0.05	⋯	⋯	0.9738	+1.73±0.60
60	0.9	⋯	0.1	⋯	⋯	0.9714	+0.63±1.07
7	0.8	⋯	0.2	⋯	⋯	0.9330	−1.37±0.40
8	0.87	⋯	⋯	0.13	⋯	1.0537	+3.02±0.35
9	0.65	⋯	⋯	0.35	⋯	1.0927	−0.83±0.40
10	0.5	⋯	⋯	0.5	⋯	1.0989	−0.83±0.35
11	0.4	⋯	⋯	0.6	⋯	1.0988	−0.81±0.40
12	0.2	⋯	⋯	0.8	⋯	1.0977	−1.45±0.43
13	0.973	⋯	⋯	⋯	0.027	0.9873	+1.96±0.28
14	0.806	⋯	⋯	⋯	0.194	0.9294	−0.58±0.40
15	0.579	⋯	⋯	⋯	0.421	0.8700	−1.45±0.35
16	0.310	⋯	⋯	⋯	0.690	0.8225	−3.19±0.40
17	0.176	⋯	⋯	⋯	0.824	0.8063	−3.23±0.36
18	0.097	⋯	⋯	⋯	0.903	0.7968	−3.22±0.38

rich regions substantially changes, from around 1 to around −1 with a decreasing water content. It is important to also notice that α_T remains negative and almost constant for $x_{\text{inethanol}} > 0.2$. This fact indicates that there is no substantial change in the degree of separation of the constituents when the water concentration decreases below about 75%. It is remarkable that our simulations are able to also reproduce this particular behavior.

Since the difference in size between methanol and ethanol is small, we may expect that their thermal diffusion factors in water solutions will be similar. Effectively, on Fig. 4 we present the variation of the thermal diffusion factor for water-ethanol mixtures versus composition at 298 K and 1 atm, in a reduced range of ethanol concentrations. Our simulation results are compared with the experimental data taken from Bou-Ali,[61] Kolodner and co-workers[9] and Sengers and co-workers[62] at the same thermodynamic conditions. Contrary to the Tichacek's data, which were published in 1956,[5] the experiments on water-ethanol mixtures have been more recently published. It is important to notice that the different sets of experimental data shown in Fig. 4 have been obtained using different techniques and are considered as reference values for this system.

As can be seen in Fig. 4, the agreement with the experimental data is excellent, better than in the water-methanol mixture. In addition, the region where the change of sign of α_T is observed is also well reproduced. The change of sign of

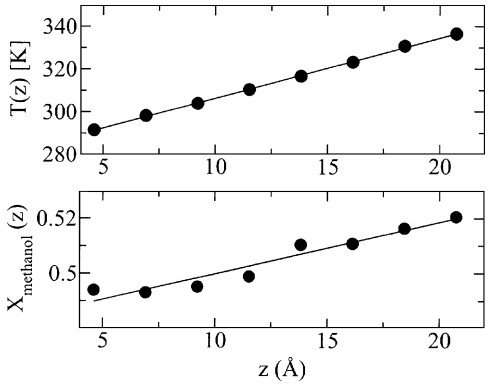

FIG. 1. Temperature profile (upper) and water concentration profile (bottom) along half of the simulation box for the water-methanol (average $X_{\text{methanol}}=0.505$) system at 313 K. Lines are obtained from a linear regression on the simulated data.

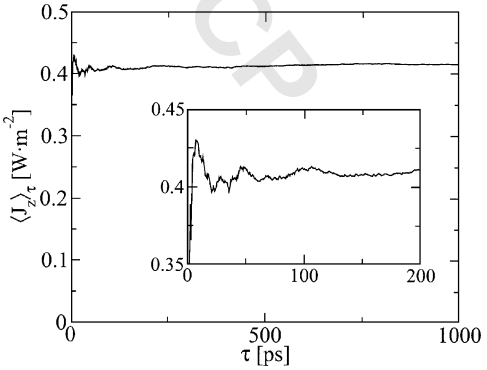

FIG. 2. Time evolution of the heat flux density [defined in Eq. (9)] in the system water-methanol (average $X_{\text{methanol}}=0.505$) system at 313 K. Inner plot shows the initial transient period, characterized by fluctuations in the heat flux density. Time origin corresponds to the beginning of the application of the PeX algorithm. The steady state of $\langle J_z \rangle_\tau$ is reached after ≈275–300 ps.

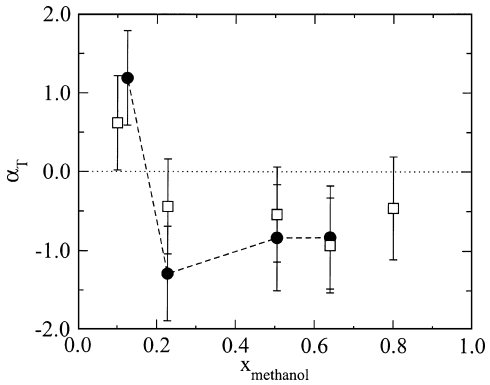

FIG. 3. Comparison of the thermal diffusion factor α_T for the water-methanol mixture vs composition at 313 K and 1 atm (●) with the experimental data of Tichacek *et al.* (Ref. 5) (□).

the thermal diffusion factor takes place for an ethanol mole fraction between 0.1 and 0.2. Unfortunately, the long simulation times required to have linear concentration profiles for the water-ethanol system was one of the main limitation encountered to compute more simulation data. Even though, we consider that our results for this mixture are very good, being the first simulations that are able to reproduce this change of sign. In view of Figs. 3 and 4, we can observe that the values of α_T obtained in both cases are qualitatively similar, though the water-ethanol system presents larger separations than the water-methanol system. Additionally, the concentration where α_T changes sign is within the same low alcohol concentration range in both cases.

In Fig. 5, we present the prediction of the thermal diffusion factor of the water-DMSO mixture versus composition at 298 K and 1 atm. Considering the good agreement obtained in the two previous water-alcohol mixtures, we expect that our predictions are good approximations of the real values.

The water-DMSO mixture is also associating and exhibits the typical features of nonideal systems of this kind, as we have found for viscosity and thermal conductivity.[57,63] Thus, we can further compare our simulation results with the values obtained with the two previous mixtures. A change of sign is again observed at water mole fraction between 0.7 and 0.8, i.e., in solutions slightly less concentrated in water

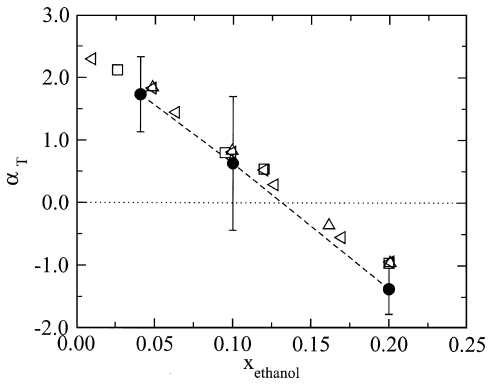

FIG. 4. Comparison of the thermal diffusion factor α_T for the water-ethanol mixture vs composition at 298 K and 1 atm (●) with the experimental data of Bou-Ali (Ref. 61) (□), Kolodner (Ref. 9) (◁), and Zhang (Ref. 62) (△).

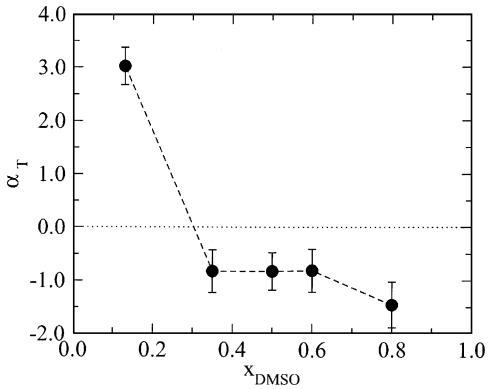

FIG. 5. Prediction of the thermal diffusion factor α_T for the water-DMSO mixture vs composition at 298 K and 1 atm.

than for water-alcohol cases. However, the results are qualitatively similar to those obtained for alcohol systems. For example, the value of the thermal diffusion factor also remains constant for DMSO mole fractions over 0.45.

Finally, in Fig. 6, we present the thermal diffusion factor data for the water-acetone mixture versus composition at 298 K and 1 atm. In this case our results should be considered as predictions, in view of the lack of experimental data on thermal diffusion for this mixture. Some aspects are worth to be mentioned. The change of sign of the thermal diffusion factor is again observed and, in addition, also in the same range of composition as for the water-alcohol mixtures, i.e., between 0.8 and 0.9 water mole fraction. However, some differences between these two types of mixtures appear. In particular, the value of α_T in the water poor region is almost three times larger than for the previous cases. Apart form this quantitative difference, the value of the coefficient also reaches a plateau in the region of low water concentration. It would be interesting to also have experimental data of this mixture to compare with the predictions done here.

V. CONCLUSIONS

In this work, we have obtained thermal diffusion coefficient in aqueous mixtures using boundary driven nonequilibrium molecular dynamics. The use of a BD-NEMD algorithm is justified by the fact that EMD plus Green–Kubo method and synthetic NEMD methods give direct access to the Onsager coefficients, the L_{ij}'s, rather than to the transport

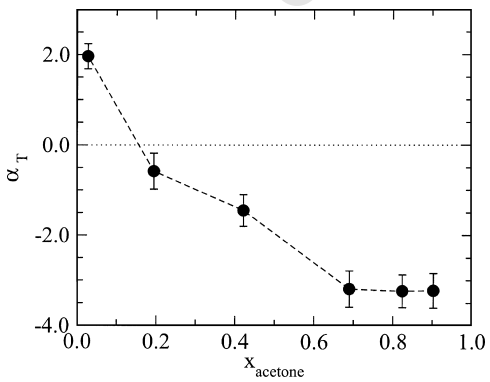

FIG. 6. Prediction of the thermal diffusion factor α_T for the water-acetone mixture vs composition at 298 K and 1 atm.

coefficients experimentally measured. In order to evaluate the experimental coefficients from the L_{ij}'s, one needs to resort to thermodynamic quantities such as partial specific enthalpies and chemical potential derivatives, difficult to obtain for such mixtures. In the case of nonideal or associated mixtures, this particular restriction may lead to wrong results. The comparison of our simulation data with reference experimental data on water-ethanol mixtures is excellent and validates the methodology employed here. We have contributed to provide a consistent methodology able to reproduce and predict the value of the thermal diffusion factor when the composition of the constituents in the systems is changed. We believe that the BD-NEMD method is able to provide quantitative values of the thermal diffusion factor of real nonideal aqueous solutions. It would be of a great interest to have a set of data for the water-acetone and water-DMSO systems to validate our results on these systems and confirm our hypothesis.

We can summarize here some remarkable aspects of the behavior of the four mixtures presented in this work. First of all, the change in the sign of the thermal diffusion factor always occurs at water rich compositions in agreement with experimental data. The composition at which this change of sign is observed is also well reproduced. At low water compositions, α_T reaches a plateau with a negative value, meaning that water, the lighter component (for all mixtures) enriches at the cold side, according to the sign convention usually taken. All systems behave qualitatively in the same way, although a much larger separation (α_T less than -3) is observed in the water-acetone mixture at low water concentration. Additionally, it seems that the differences in the molar masses between all solutes play a minor role in the final value of the thermal diffusion factor, contrary to what is observed for normal nonassociating liquid mixtures. Note, for instance, that the molar mass of DMSO is 78 g/mol more than twice the molar mass of methanol of 32 g/mol. This clearly indicates that the so-called *chemical effect* dominates the behavior of the Soret coefficient in the systems studied here.

Our work, together with many other works on aqueous solutions, raises again the point of the great difficulty in the physical explanation of the particular behavior of aqueous solutions, especially those that are able to form hydrogen bonds with water. In a recent work we gave a qualitative explanation of the nature of the change of sign observed[23] in associating systems. Effectively, if one considers that the interspecies interactions are strong and in fact dominate over the intraspecies interactions, it is thus rather straightforward to see that the diluted component is always the more strongly bound to the environment and, therefore, will concentrate at the cold side of the box. Nevertheless, much more work needs to be done to eventually acquire a complete understanding of the peculiar behavior of water as solvent.

ACKNOWLEDGMENTS

This study was supported by the Spanish Government *Ministerio de Eduacin, Ciencia y Deporte* (Grant No. CTQ2004-03346/PPQ) *Generalitat de Catalunya* (Project Nos. ACI2000-13, ACI2001-39, and ACI2002-37) and the URV (Project No. 2000PIR-21). C.N.-D. thanks the Universitat Rovira i Virgili and *Ministerio de Educacion Cultura y Deporte* (Spain) for financial support. B.R. thanks the CRI, Université Paris-Sud 11 for a generous allocation of computer time.

[1] S. Chapman and T. G. Cowling, *The Mathematical Theory of Non-Uniform Gases*, 3rd ed. (Cambridge University Press, Cambridge, 1970).
[2] C. Debuschewitz and W. Köhler, Phys. Rev. Lett. **87**, 055901 (2001).
[3] D. Longree, J. C. Legros, and G. Thomaes, J. Phys. Chem. **84**, 3480 (1980).
[4] A. Perronace, C. Leppla, F. Leroy, B. Rousseau, and S. Wiegand, J. Chem. Phys. **116**, 3718 (2002).
[5] L. J. Tichacek, W. S. Kmak, and H. G. Drickamer, J. Phys. Chem. **60**, 660 (1956).
[6] I. Prigogine, L. de Brouckère, and R. Amand, Physica (Amsterdam) **16**, 577 (1950).
[7] I. Prigogine, L. de Brouckère, and R. Amand, Physica (Amsterdam) **16**, 851 (1950).
[8] H. J. V. Tyrrell, *Diffusion and Heat Flow in Liquids* (Butterworths, London, 1961).
[9] P. Kolodner, H. Williams, and C. Moe, J. Chem. Phys. **88**, 6512 (1988).
[10] R. Piazza and A. Guarino, Phys. Rev. Lett. **88**, 208302 (2002).
[11] R. Piazza, Philos. Mag. **83**, 2067 (2003).
[12] S. Iacopini and R. Piazza, Europhys. Lett. **63**, 247 (2003).
[13] C. Leppla and S. Wiegand, Philos. Mag. **83**, 1989 (2003).
[14] B. de Gans, B. M. R. Kita, and S. Wiegand, J. Chem. Phys. **118**, 8073 (2003).
[15] B. de Gans, S. Wiegand, and J. Luettmer-Strathman, Phys. Rev. Lett. **91**, 245501 (2003).
[16] R. Kita, G. Kircher, and S. Wiegand, J. Chem. Phys. **121**, 9140 (2004).
[17] R. Kita, S. Wiegand, and J. Luettmer-Strathman, J. Chem. Phys. **121**, 3874 (2004).
[18] R. Haase, Z. Phys. **127**, 1 (1950).
[19] E. L. Dougherty and H. G. Drickamer, J. Phys. Chem. **59**, 443 (1955).
[20] J. M. Kincaid, E. G. D. Cohen, and M. L. de Haro, J. Chem. Phys. **86**, 963 (1987).
[21] L. J. T. M. Kempers, J. Chem. Phys. **90**, 6541 (1989).
[22] L. J. T. M. Kempers, J. Chem. Phys. **115**, 6330 (2001).
[23] B. Rousseau, C. Nieto-Draghi, and J. B. Àvalos, Europhys. Lett. **67**, 976 (2004).
[24] S. R. de Groot and P. Mazur, *Non-Equilibrium Thermodynamics* (North-Holland, Amsterdam, 1969).
[25] R. Vogelsang, C. Hoheisel, G. Paolini, and G. Ciccotti, Phys. Rev. A **36**, 3964 (1987).
[26] R. Vogelsang and C. Hoheisel, J. Chem. Phys. **89**, 1588 (1988).
[27] D. MacGowan and D. J. Evans, Phys. Rev. A **34**, 2133 (1986).
[28] S. Sarman and D. J. Evans, Phys. Rev. A **45**, 2370 (1992).
[29] S. Sarman and D. J. Evans, Phys. Rev. A **45**, 2370 (1992).
[30] G. V. Paolini and G. Ciccotti, Phys. Rev. A **35**, 5156 (1987).
[31] D. L. Jolly and R. J. Bearman, Mol. Phys. **41**, 137 (1980).
[32] M. Schoen and C. Hoheisel, Mol. Phys. **52**, 33 (1984).
[33] J. M. Stoker and R. L. Rowley, J. Chem. Phys. **91**, 3670 (1989).
[34] J. H. Irving and J. G. Kirkwood, J. Chem. Phys. **18**, 817 (1950).
[35] F. Müller-Plathe, J. Chem. Phys. **106**, 6082 (1997).
[36] D. Bedrov and G. D. Smith, J. Chem. Phys. **113**, 8080 (2000).
[37] C. Nieto-Draghi and J. B. Avalos, Mol. Phys. **101**, 2303 (2003).
[38] H. Goldstein, *Classical Mechanics* (Addison-Wesley, Massachusetts, 1996).
[39] H. M. Schaink and C. Hoheisel, Physica A **184**, 451 (1992).
[40] H. M. Schaink, H. Luo, and C. Hoheisel, J. Chem. Phys. **99**, 9912 (1993).
[41] J.-M. Simon, D. K. Dysthe, A. H. Fuchs, and B. Rousseau, Fluid Phase Equilib. **150–151**, 151 (1998).
[42] J.-M. Simon, B. Rousseau, D. K. Dysthe, and B. Hafskjold, Entropie **217**, 29 (1999).
[43] A. Perronace, G. Ciccotti, F. Leroy, A. H. Fuchs, and B. Rousseau, Phys. Rev. E **66**, 031201 (2002).
[44] W. Jorgensen, J. Phys. Chem. **90**, 1276 (1986).
[45] W. Jorgensen, J. Chandrasekhar, J. D. Madura, R. W. Impey, and M. Klein, J. Chem. Phys. **79**, 926 (1983).
[46] C. Benmore and Y. L. Loh, J. Phys. Chem. **112**, 5877 (2000).
[47] A. Shevade and K. E. Gubbins, J. Phys. Chem. **113**, 6933 (2000).

[48]M. Matsumoto and K. E. Gubbins, J. Chem. Phys. **93**, 1981 (1990).
[49]L. Saiz, J. A. Padró, and E. Guárdia, Mol. Phys. **97**, 897 (1999).
[50]J. T. Slusher, Mol. Phys. **98**, 287 (2000).
[51]G. Sesé and R. Palomar, J. Phys. Chem. **114**, 9975 (2001).
[52]J. Petravic and J. Delhommelle, Chem. Phys. **286**, 303 (2003).
[53]A. Luzar and D. Chandler, J. Chem. Phys. **98**, 8160 (1993).
[54]H. J. C. Berendsen, J. R. Grigera, and T. P. Straasma, J. Phys. Chem. **91**, 6269 (1987).
[55]I. A. Borin and M. S. Skaf, J. Chem. Phys. **110**, 6412 (1999).
[56]M. S. Skaf, J. Phys. Chem. A **103**, 10719 (1999).
[57]C. Nieto-Draghi, J. Bonet, and B. Rousseau, J. Chem. Phys. **119**, 4782 (2003).
[58]D. R. Wheeler and R. L. Rowley, Mol. Phys. **94**, 555 (1998).
[59]M. Neuman, J. Chem. Phys. **85**, 1567 (1986).
[60]M. P. Allen and D. J. Tildesley, *Computer Simulation of Liquids*, 1st ed. (Clarendon, Oxford, 1989).
[61]M. M. Bou-Ali, Ph.D. thesis, Universidad del Pais Vasco, 1999.
[62]K. J. Zhang, M. E. Briggs, R. W. Gammon, and J. W. Sengers, J. Chem. Phys. **104**, 6881 (1996).
[63]C. Nieto-Draghi, J. B. Avalos, and B. Rousseau (unpublished).
[64]GOWPROP-v5.1, Norcraft Software, 2002.
[65]J. M. G. Cowie and P. M. Toporowski, Can. J. Chem. **39**, 2240 (1961).
[66]V. S. Griffiths, J. Chem. Soc. ■, 1326 (1952).